AFRL-RZ-WP-TP-2012-0130

FLUX PINNING OF Y-Ba-Cu-O FILMS DOPED WITH $BaZrO_3$ NANOPARTICLES BY MULTILAYER AND SINGLE TARGET METHODS (POSTPRINT)

Timothy J. Haugan, Paul N. Barnes, Timothy A. Campbell, and Neal A. Pierce

Mechanical Energy Conversion Branch
Energy/Power/Thermal Division

F. Javier Baca

Los Alamos National Laboratory

Iman Maartense

University of Dayton Research Institute

FEBRUARY 2012

AIR FORCE RESEARCH LABORATORY
PROPULSION DIRECTORATE
WRIGHT-PATTERSON AIR FORCE BASE, OH 45433-7251
AIR FORCE MATERIEL COMMAND
UNITED STATES AIR FORCE

REPORT DOCUMENTATION PAGE

Form Approved
OMB No. 0704-0188

1. REPORT DATE *(DD-MM-YY)*	2. REPORT TYPE	3. DATES COVERED *(From - To)*
February 2012	Journal Article Postprint	04 April 2005 – 04 April 2007

4. TITLE AND SUBTITLE

FLUX PINNING OF Y-Ba-Cu-O FILMS DOPED WITH $BaZrO_3$ NANOPARTICLES BY MULTILAYER AND SINGLE TARGET METHODS (POSTPRINT)

5a. CONTRACT NUMBER
In-house

5b. GRANT NUMBER

5c. PROGRAM ELEMENT NUMBER
62203F

6. AUTHOR(S)

Timothy J. Haugan, Paul N. Barnes, Timothy A. Campbell, and Neal A. Pierce (AFRL/RZPG)

F. Javier Baca (Los Alamos National Laboratory)

Iman Maartense (University of Dayton Research Institute)

5d. PROJECT NUMBER
3145

5e. TASK NUMBER
32

5f. WORK UNIT NUMBER
314532ZE

7. PERFORMING ORGANIZATION NAME(S) AND ADDRESS(ES)

Mechanical Energy Conversion Branch (AFRL/RZPG)
Energy/Power/Thermal Division
Air Force Research Laboratory, Propulsion Directorate
Wright-Patterson Air Force Base, OH 45433-7251
Air Force Materiel Command, United States Air Force

Los Alamos National Laboratory
Los Alamos, NM 87545

University of Dayton Research Institute
Dayton, OH 45469

8. PERFORMING ORGANIZATION REPORT NUMBER
AFRL-RZ-WP-TP-2012-0130

9. SPONSORING/MONITORING AGENCY NAME(S) AND ADDRESS(ES)

Air Force Research Laboratory
Propulsion Directorate
Wright-Patterson Air Force Base, OH 45433-7251
Air Force Materiel Command
United States Air Force

10. SPONSORING/MONITORING AGENCY ACRONYM(S)
AFRL/RZPG

11. SPONSORING/MONITORING AGENCY REPORT NUMBER(S)
AFRL-RZ-WP-TP-2012-0130

12. DISTRIBUTION/AVAILABILITY STATEMENT

Approved for public release; distribution unlimited.

13. SUPPLEMENTARY NOTES

Journal article published in *IEEE Transactions on Applied Superconductivity*, Vol. 17, No. 2, June 2007.

PA Case Number: AFRL/WS 06-0233; Clearance Date: 04 Apr 2007.

Work on this effort was completed in 2007.

14. ABSTRACT

The superconducting properties of $YBa_2Cu_3O_{7-x}$ (YBCO or 123) thin films doped with $BaZrO_3$ (BZO) nanoparticles by multilayer and single-target methods were studied and compared. Thin films of 123 + BZO were processed by pulsed laser deposition on $LaAlO_3$ and $SrTiO_3$ single crystal substrates. Multilayer $(BZO_{0.6\ nm-1.4\ nm}/23_{15\ nm})_{19}$ structures were grown by alternating deposition from 123 and BZO targets, and BZO additions of 0–2 Vol% were deposited using $(123_{1-x}\ BZO_x)$ single-targets. The multilayer and single-target methods of BZO addition caused significant differences of superconducting transition temperatures (T_c) measured by AC susceptibility, and critical current densities (J_c) measured by both magnetic and transport methods as a function of temperature (T), applied magnetic field (H) and angle of H field incidence (θ). Single-target films had almost linear decrease of T_c and self-field J_c with BZO vol% addition, and compared to multilayer films had lower J_c(77 K, H < 4 T) however had improved high-field properties for J_c(77 K, H >4 T). Multilayer films had almost no decrease of T_c and self-field J_c for high BZO additions up to 10 Vol% and very strong peak of J_c(H / / ab in – plane) and constant and high J_c(H, < 0 80°). Single-target BZO-2 Vol% films had slightly enhanced J_c(H / /c – axis), consistent with results by other authors.

15. SUBJECT TERMS

superconducting, magnetic field, critical current densities, pulsed laser deposition, nanoparticles, multilayer, substrates

16. SECURITY CLASSIFICATION OF:			17. LIMITATION OF ABSTRACT:	18. NUMBER OF PAGES	19a. NAME OF RESPONSIBLE PERSON (Monitor)
a. REPORT	b. ABSTRACT	c. THIS PAGE			Timothy J. Haugan
Unclassified	Unclassified	Unclassified	SAR	12	19b. TELEPHONE NUMBER *(Include Area Code)* N/A

Flux Pinning of Y-Ba-Cu-O Films Doped With $BaZrO_3$ Nanoparticles by Multilayer and Single Target Methods

Timothy J. Haugan, *Member, IEEE*, Paul N. Barnes, Timothy A. Campbell, Neal A. Pierce, F. Javier Baca, and Iman Maartense

***Abstract*—The superconducting properties of $YBa_2Cu_3O_{7-x}$ (YBCO or 123) thin films doped with $BaZrO_3$ (BZO) nanoparticles by multilayer and single-target methods were studied and compared. Thin films of $123 + BZO$ were processed by pulsed laser deposition on $LaAlO_3$ and $SrTiO_3$ single crystal substrates. Multilayer $(BZO_{0.6\ nm-1.4\ nm}/123_{15\ nm})_{19}$ structures were grown by alternating deposition from 123 and BZO targets, and BZO additions of 0–2 Vol% were deposited using $(123_{1-x}BZO_x)$ single-targets. The multilayer and single-target methods of BZO addition caused significant differences of superconducting transition temperatures (T_c) measured by AC susceptibility, and critical current densities (J_c) measured by both magnetic and transport methods as a function of temperature (T), applied magnetic field (H) and angle of H field incidence (θ). Single-target films had almost linear decrease of T_c and self-field J_c with BZO vol% addition, and compared to multilayer films had lower $J_c(77\ K, H < 4\ T)$ however had improved high-field properties for $J_c(77\ K, H > 4\ T)$. Multilayer films had almost no decrease of T_c and self-field J_c for high BZO additions up to 10 Vol% and very strong peak of $J_c(H//ab\ in-plane)$ and constant and high $J_c(H, 0 < \theta < 80°)$. Single-target BZO-2 Vol% films had slightly enhanced $J_c(H//c-axis)$, consistent with results by other authors.**

***Index Terms*—Flux pinning, nanoparticle, superconductor, thin film, $YBa_2Cu_3O_{7-x}$.**

I. Introduction

THE development of high temperature superconductor $YBa_2Cu_3O_{7-\delta}$ (YBCO or 123) thin films on polycrystalline substrates (coated conductors) with $J_c > 1\ MA/cm^2$ offers great promise for incorporation into power applications such as generators or motors, operating at 77 K [1]–[5]. YBCO has excellent properties at 77 K including high $J_c(H)$ due to strong flux pinning. However it is of interest to increase $J_c(H)$ even further to increase wire performance and reduce production costs [1], [2]. For type-II superconductors, it is known that flux pinning can be increased by incorporating a high density of extended non-superconducting defects into the material [2]–[4]. The defect size should be approximately the coherence length ~2–4 nm at 4.2–77 K to maximize pinning [2]–[4].

Manuscript received August 29, 2006. This work was supported in part by the U.S. Air Force Office of Scientific Research and the Air Force Research Laboratory—Propulsion Directorate.

The authors are with the Air Force Research Laboratory, Propulsion Directorate-AFRL/PRPG, Wright Patterson AFB, OH 45433-7251 USA (e-mail: timothy.haugan@wpafb.af.mil).

Color versions of one or more of the figures in this paper are available online at http://ieeexplore.ieee.org.

Digital Object Identifier 10.1109/TASC.2007.899342

Many methods of introducing defects have been considered to increase flux pinning in YBCO, and recent efforts have focused on addition of ~3–20 nm size nanoparticles by multilayer [5]–[16] and single-target methods [12], [17]–[21]. For multilayer $(M_n/123_m)N$ films, a number of different second-phase additions M have been studied including $M = green-phase\ Y_2BaCuO_5$ (Y211) [5]–[12], Y_2O_3 [11], [12], [14], [15], CeO_2 [11]–[13], $IrZrO_3$ [16], and other phases with negative effects on T_c and/or $J_c(H)$ including $M = La211$ [11], [12], MgO [11], [12], and Sm123 [12]. For $(RE123_{1-x}M_x)$ single-target films with $RE = Y$, Sm, and other rare-earths, a number of materials have been considered that provided increases of flux pinning including $M = BZO$ [12], [17]–[19], excess RE and Cu [21], and minute dopants such as Tb, Nd, and Pr [20].

For nanoparticle M phase additions in $(M_n/123_m)_N$ multilayer films, both the lattice-mismatch and chemical reactivity are understood to play important roles to provide effective pinning centers [11], [12]. A non-reactive material is desired to prevent diffusion and poisoning of T_c [11], [12]. High lattice-mismatched materials such as Y211 (5%) provide good pinning for large 123 layer spacing such as $m = 10$–15 nm, however for medium lattice-mismatched materials such as Y_2O_3 (−2.5%) a very thin Y123 layer spacing $m < 5$ nm is required to provide significant increase of $J_c(H)$ compared to Y123-only reference films [12]. For very low lattice-mismatched materials including CeO_2 and Sm123 (−0.7% and +0.6%, respectively), the decrease of $J_c(H > 0.5\ T)$ is almost 10–100 times compared to Y123-only regardless of the Y123 layer spacing thickness m, which strongly suggests effective flux pinning defects are being eliminated with growth of a too-perfect film structure [11]–[13].

Because of excellent success with high lattice-mismatched materials such as Y211 with ~5%, it was considered an important next step to study pinning materials with similar or greater lattice mismatch, such as BZO (+8.7%) or MgO (+9.6%). MgO was shown to be highly reactive and cause a strong broadening and decrease T_c for even low volume % additions [11], [12]. In contrast BZO was shown to be mostly non-reactive and effective for pinning in single-target films [12], [17]–[19].

In this paper, $M = BZO$ was chosen as a next candidate to study in $(M_n/123_m)_N$ multilayer films. Also in this paper, the properties of $(BZO_n/123_m)_N$ multilayer films were studied and compared directly to $(123_{1-x}BZO_x)$ single-target films, to provide a first-time comparison of same-phase defect addition by multilayer and single-target methods. All multilayer films in this

study were $\sim 0.25-0.35\ \mu\mathrm{m}$ thickness to reduce thickness-dependent variation of J_c, and also deposited on single crystal substrates to provide a comparison to previous results [5]–[16]. Excellent results for $(123_{1-x}BZO_x)$ single-target films have been published previously, however these studies were done on buffered-metallic substrates or for $> 1\ \mu\mathrm{m}$ thick films and could not be used for the comparisons studied herein [17]–[19].

II. Experimental

Multilayer $(BZO_n/123_{15\ nm})_{19}$ and $(123_{1-x}BZO_x)$ films were deposited by pulsed laser deposition (PLD), using parameters and conditions described in detail previously [5]–[12], [22]. Deposition parameters were 248 nm laser wavelength, $\sim 3.2\ \mathrm{J/cm^2}$ laser fluence, 25 nm pulse length, 2–4 Hz laser repetition rate, 5.5 cm target-to-substrate distance, 775–790°C heater block temperature, 83–90% dense targets, 300 mTorr oxygen partial-pressure, and a post-deposition anneal at 500°C and 1 atmosphere of oxygen [22]. Substrates were $LaAlO_3$ (LAO) and $SrTiO_3$ (STO) 100 oriented single crystals, with epi-polish. For multilayer films, an automated target rotation and pulse-triggering system was used to control the deposition sequences, with a period of about 13 seconds during which the deposition was stopped and different targets were rotated into position. The deposition rate for each pinning material was calibrated prior to multilayer deposition. The 'pseudo-layer' thickness in the multilayer films was calculated assuming smooth continuous film coverage, although the insulating layer in most cases consisted of discontinuous and discrete nanoparticles. Deposition rates for Y123 and $(Y123_{1-x}BZO_x)$ were 13–15 nm/min and for BZO was 30–35 nm/min. To obtain lower BZO deposition rate for multilayer films with BZO volume fraction <6%, an attenuating lens was added to reduce laser fluence by ~30%. The total film thickness was kept in the range of 0.25–0.35 μm to provide consistent comparisons. The film thickness of every sample was measured multiple times across acid-etched step-edges with a profilometer (KLA-Tencor, P15), to obtain an average value.

The superconducting transition temperature (T_c) was measured using an AC susceptibility technique with the amplitude of the magnetic sensing field strength, h, varied from 0.025–2.2 Oe, at a frequency of approximately 4 Hz. Note that the AC susceptibility technique provides information about primary and secondary transitions of the entire film, rather than a defined path that is obtained with transport T_c measurements. Magnetic J_c measurements were made with a vibrating sample magnetometer (VSM) in magnetic field strengths of 0 to 9 T, and a ramp rate of 0.01 $(T \bullet s^{-1})$. The J_c of the square samples was estimated using a simplified Bean model $J_c = 15\Delta M/R$, where M is magnetization/volume from M-H loops, and R is the radius of volume interaction = square side for consistency [12]. Characterization of microstructures was performed with scanning electron microscopy in ultra-high resolution mode (SEM, FEI-Sirion). Transport J_c measurements were made with microbridges 0.03–0.05 cm wide by 0.3 cm length by 4-point contact method, and with voltage criteria of 1 $\mu\mathrm{V/cm}$. Microbridges were made by 248 nm UV laser etching through alumina masks with laser fluence 0.1 $\mathrm{J/cm^2}$, laser pulse length 25 ns, and at 1 Hz. The critical current was measured in liquid nitrogen at 77.2 K. Current was applied to the sample by a step-ramp method: a current step interval of 0.2–0.5 s, a ramp rate of 0.25–1.0 A/s, and a voltage sample period 2–4 times smaller than the current step interval. The maximum current step size was 0.1 A.

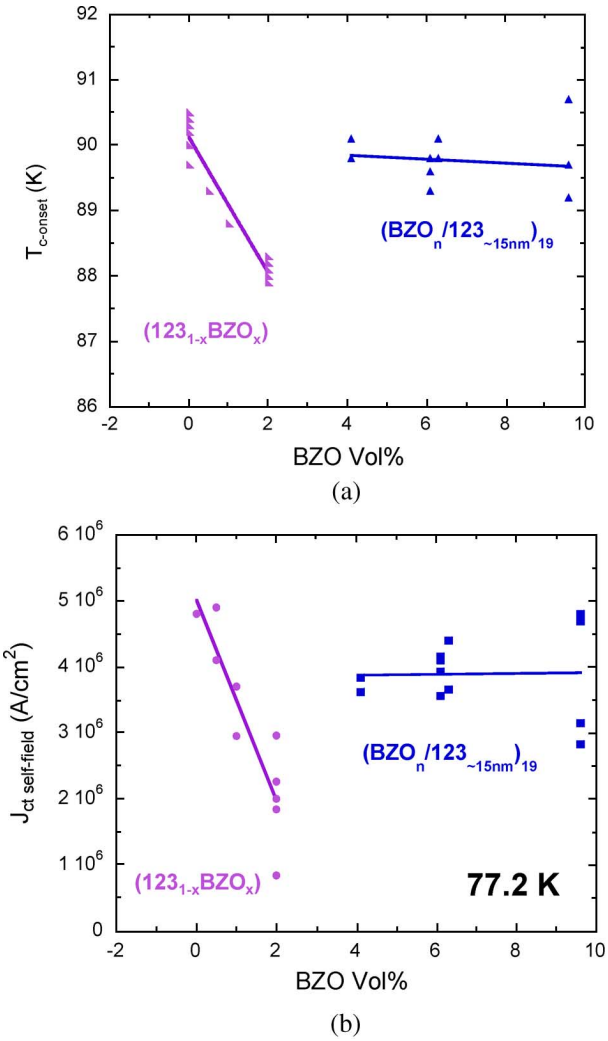

Fig. 1. Superconducting properties of BZO films made by single-target and $(BZO_n/123_{15\ nm})_{19}$ multilayer structures, as a function of BZO volume percent addition. The plots demonstrate a significant difference between multilayer and single-target films, with multilayer films having much less effect on T_c and self-field J_c for significantly larger volume % BZO addition. (a) T_c onset by ac susceptibility. T_c transition widths for all films were comparable in the range of 1.5 K to 2 K. (b) Self-field J_c measured by transport methods.

III. Results

The effect of BZO addition on T_c and self-field $J_c(J_{c-sf})$ are shown in Fig. 1, for both multilayer and single-target films. As seen in Fig. 1, BZO addition for single-target films had a strong negative effect with both T_c and J_{c-sf} decreasing almost linearly with increasing volume % addition of BZO. It is possible to correlate the decrease of J_{c-sf} with the decrease of T_c, however the T_c transitions were still narrow about 1.5–2 K for BZO-2 Vol% addition, so it is assumed other mechanisms are affecting J_{c-sf} such as decreasing superconducting volume fraction, cation disorder, or slight poisoning.

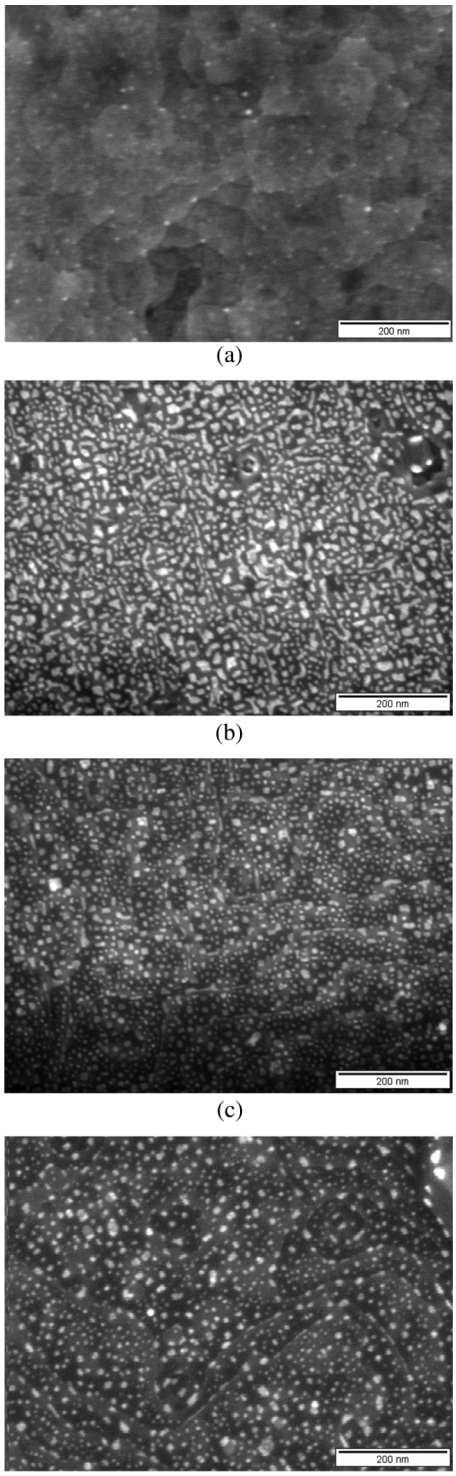

Fig. 2. SEM micrographs of $123+\mathrm{BZO}$ film surfaces, obtained with ultra-high resolution focus at 150,000× magnification. Insulating phases are (white or lighter) color from enhanced surface charging and emission of imaging electrons. Note the unusual decoration of ledges in (c) and (d). Because of different lattice-mismatch and epitaxy mechanism, BZO has different island-growth than 211, $\mathrm{Y_2O_3}$, or $\mathrm{CeO_2}$ forming ∼35% smaller nanoparticle size and $\sim 3-4\times$ higher areal number densities [5], [6], [14]. $\mathrm{Nanoparticle\ size} = 7.5\ \mathrm{nm_{Avg}} \pm 2.2\ \mathrm{nm_{Stdev}}$ for (c) and $8.8\ \mathrm{nm_{Avg}} \pm 3.5\ \mathrm{nm_{Stdev}}$ for (d), and $\mathrm{areal\ number\ densities} = 4.9 \times 10^{11}\ \mathrm{nanoparticles} \bullet \mathrm{cm}^{-2}$ for (c) and $3.4 \times 10^{11}\ \mathrm{nanoparticles} \bullet \mathrm{cm}^{-2}$ for (d). (a) $(123_{0.98}\mathrm{BZO}_{0.02})/\mathrm{LAO}$; (b) $(\mathrm{BZO}_{1.6\ \mathrm{nm}}/123_{15\ \mathrm{nm}})_{19}/\mathrm{STO}$; (c) $(\mathrm{BZO}_{1.0\ \mathrm{nm}}/123_{15\ \mathrm{nm}})_{19}/\mathrm{STO}$; (d) $(\mathrm{BZO}_{0.7\ \mathrm{nm}}/123_{15\ \mathrm{nm}})_{19}/\mathrm{LAO}$.

In contrast to single-target films, multilayer films showed almost no decrease of $\mathrm{T_c}$ and $\mathrm{J_{c-sf}}$ even with large BZO volume fraction additions up to 10%. The reason for the strong difference for multilayer films especially of $\mathrm{T_c}$ is unknown, however possibly is a result of less Zr diffusion and poisoning. Maintaining almost maximum $\mathrm{J_{c-sf}}$ for large BZO coverage ∼1.4 nm (10 Vol%) is significantly different from previous studies of $(\mathrm{CeO_2}/123)_\mathrm{N}$ multilayer structures, where $\mathrm{J_{c-sf}}$ reduced almost to 1–2 $\mathrm{MA/cm^2}$ for similar insulating layer coverage. The difference of these results is that BZO with lattice mismatch +8.7% may cause stress related defects that increase $\mathrm{J_c}$, whereas $\mathrm{CeO_2}$ is a very close lattice mismatch −0.7% which makes the YBCO growth too perfect and reduces $\mathrm{J_c}$ because of decrease of pinning defects.

The effect of BZO additions on microstructures is shown in Fig. 2 for both single-target and multilayer films, as imaged by SEM on film surfaces at high 150,000× magnification. Small nanoparticles <5 nm size with high volumic number density were observed for BZO-2 Vol% in single-target films, consistent with previous authors [17]–[19]. For multilayer $(\mathrm{BZO}/123)_\mathrm{N}$ films, as the BZO surface layer coverage increased from 0.7 nm to 1.0 nm the nanoparticle formations increased in areal number density ∼35% while maintaining approximately the same size of 7–9 nm. As the BZO 'pseudo-layer' thickness increased to 1.6 nm, the nanoparticle size increased significantly simultaneous with a decrease of areal number density ∼35%. For multilayer films with BZO $\mathrm{n} = 1.0\ \mathrm{nm}$ the average nanoparticle size was $\mathrm{small} = 7.5\ \mathrm{nm}$, and the areal number density was $\mathrm{very\ high} = 5 \times 10^{11}\ \mathrm{nanoparticles} \bullet \mathrm{cm}^{-2}$ which was ∼3–4 times greater than areal number densities for optimized $\mathrm{Y_2O_3}$ or Y211 monolayers [5], [6], [14]. This indicates the island-growth formation mechanisms are significantly different for BZO than Y211 or $\mathrm{Y_2O_3}$. This growth difference may have advantages to increase pinning uniformity or strength.

The effect of BZO additions on $\mathrm{J_c(H, 65\ K - 77\ K)}$ were measured by magnetic and transport methods in Fig. 3 and Fig. 4, respectively. As shown in Fig. 3, for $(\mathrm{BZO}/123)_\mathrm{N}$ multilayer films the lowest coverage of BZO tested thus far ($\mathrm{BZO} = 0.7\ \mathrm{nm}$ or 4 Vol%) had the highest $\mathrm{J_c(H//c-axis)}$. This is consistent with previous studies of $(\mathrm{M}/123)_\mathrm{N}$ films, where minimization of the M surface coverage was necessary to maximize $\mathrm{J_c(H//c-axis)}$ [11], [13]. In Fig. 3, $\mathrm{J_{cm}(H//c-axis)}$ properties of a $(123_{0.98}\mathrm{BZO}_{0.02})$ film compared to $(\mathrm{BZO}/123)_\mathrm{N}$ films were slightly better at 65 K and noticeably higher at 77 K for $\mathrm{H} > 3\ \mathrm{T}$. Trends of $\mathrm{J_c(77\ K, H)}$ in Fig. 3 for magnetic measurements were also confirmed by transport measurements in Fig. 4. For multilayer films the smallest BZO layer tested ($\mathrm{BZO} = 0.9\ \mathrm{nm}$) had the highest $\mathrm{J_{ct}(H)}$ properties. Compared to a $(123_{0.98}\mathrm{BZO}_{0.02})$ film this best multilayer film had slight enhancement of $\mathrm{J_c(77\ K, H < 4\ T)}$ but was reduced for $\mathrm{J_c(77\ K, H > 4\ T)}$.

The angular dependence of $\mathrm{J_c(H = 1\ T)}$ was studied for both multilayer and single-target films in Fig. 5. In Fig. 5, a BZO-2 Vol% single-target film had a slightly enhanced $\mathrm{J_c(H//c-axis)}$ peak, consistent with results by previous authors [17]–[19]. The $\mathrm{J_c(H//ab-plane)}$ for the $(\mathrm{BZO}/123)_\mathrm{N}$ multilayer film was quite high and about 3× higher than measurements for a similar $(211/123)_\mathrm{N}$ multilayer film. We believe this provides evidence

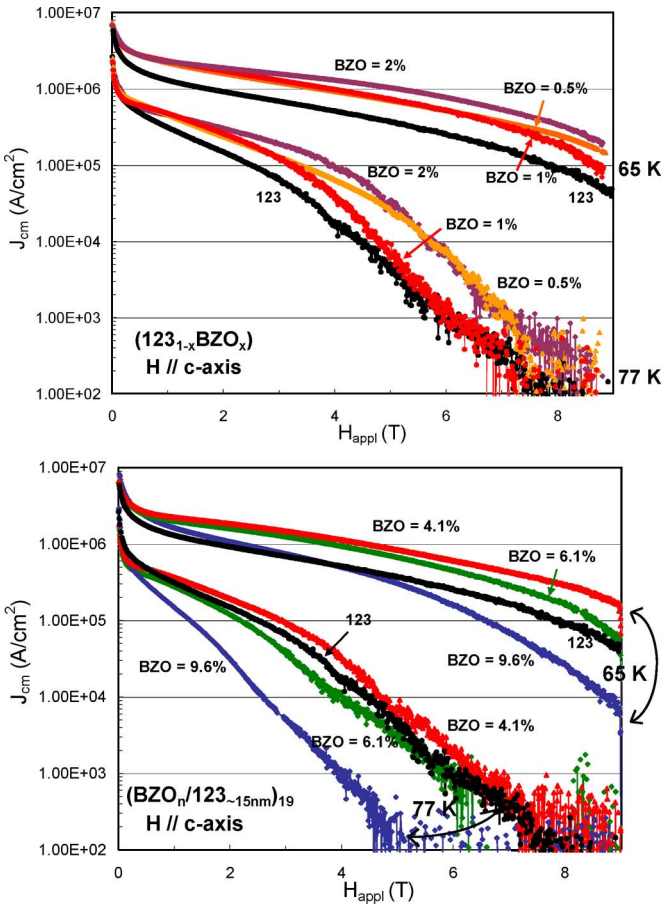

Fig. 3. Critical current density measured by magnetic methods for varying BZO Vol % addition: (upper) single-target $(123_{1-x}BZO_x)$ films, and (lower) $(BZO_n/123)_{19}$ multilayer films. Despite lower self-field J_c, single-target $(123_{1-x}BZO_x)$ films generally have increased $J_c(H)$ compared to $(BZO_n/123)_{19}$ multilayer films. However $(BZO/123)_N$ multilayer films have not been fully optimized yet, as lower BZO content could potentially further increase $J_c(H)$. Results of $J_{cm}(H)$ were consistent for both LAO and STO substrates.

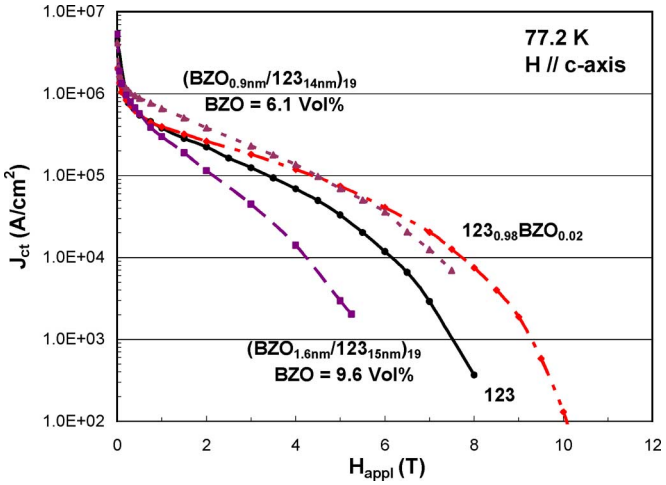

Fig. 4. Critical current density measured by transport methods at 77 K. Relative trends of $J_c(H)$ measured by magnetic methods in Fig. 3 are further confirmed. The $J_c(H)$ for the $(BZO_{0.9\ nm}/123_{14\ nm})_{19}$ multilayer film is higher than $(123_{1-x}BZO_x)$ for $H < 4$ T mostly because of increased self-field $J_c \sim 4\ MA/cm^2$ compared to $\sim 2\ MA/cm^2$. For multilayer films, surface layer coverage for BZO ~ 1.6 nm (BZO $-$ Vol% $= 9.6\%$) is too high which reduces $J_c(H)$ compared to BZO ~ 0.9 nm.

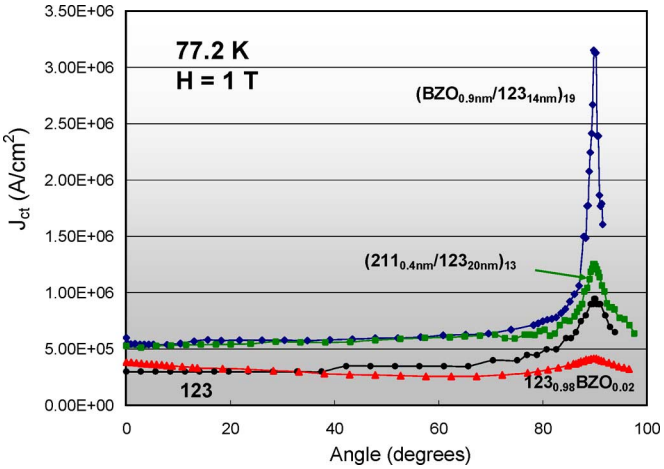

Fig. 5. Critical current density for $H_{appl} = 1$ T as a function of H incidence angle: $\theta = 0$ for H//c-axis. $J_c(1\ T, \theta = 90°)$ for $(BZO_{0.9\ nm}/123_{14\ nm})_{19}$ multilayer film $(BZO - Vol\% = 6.1\%)$ is $\sim 3\times$ higher than a similar multilayer with Y211 instead of BZO. Enhancement of the c-axis peak for $(123_{1-x}BZO_x)$ is consistent with results of previous authors [17]–[19].

the nanoparticle coverage is more uniform and consistent for BZO than 211.

IV. Conclusions

It was demonstrated that BZO nanoparticle additions by multilayer or single-target methods had strong and somewhat surprisingly different effects on superconducting properties including T_c, self-field J_c, and $J_c(H, T, \theta)$ as measured by both transport and magnetic methods. Addition of BZO in $(123_{1-x}BZO_x)$ single-target films strongly decreased T_c and self-field J_c almost linearly with BZO-Vol% addition. By comparison BZO additions up to 10 Vol% in $(BZO_n/123_{15\ nm})_{19}$ multilayer films had almost no effect on T_c and self-field J_c. However despite lower T_c and self-field J_c, $J_c(H > 4\ T)$ was increased significantly for single-target BZO-2 Vol% compared to BZO-4–6 Vol% multilayer films. Optimization of $(BZO/123)_N$ multilayer films has not been completed, requiring further reduction of BZO layer coverage and optimization of 123 layer thickness.

Surface layer coverage of the M insulating layer of $(M/123)_N$ multilayer films was significantly different for $M = BZO$ than $M = Y211$ and Y_2O_3 studied previously [5]–[12], with small nanoparticle size $\sim$8 nm and $\sim$3–4 times higher nanoparticle areal number density achieved $(5\times10^{11}\ nanoparticles \bullet cm^{-2})$ for BZO. This different layer coverage could have important advantages for improving flux pinning uniformity and strength, as already demonstrated by a $\sim 3\times$ increase of $J_c(H//ab-plane)$ in this study. Further testing and optimization may demonstrate additional advantages.

Acknowledgment

The authors would like to express appreciation to Lyle Brunke, John Murphy, Joseph Kell, Mary Locke, David Blubaugh, Patrick Klenk, and Randall Morgan for assistance with $J_c(H, T, \theta)$ and film thickness measurements.

REFERENCES

[1] P. N. Barnes, M. D. Sumption, and G. L. Rhoads, "Review of high power density superconducting generators: Present state and prospects for incorporating YBCO windings," *Cryogenics*, vol. 45, pp. 670–686, 2005.

[2] D. Larbalestier, A. Gurevich, D. M. Feldmann, and A. Polyanskii, "High- $\mathrm{T_c}$ superconducting materials for electric power applications," *Nature*, vol. 414, pp. 368–377, 2001.

[3] T. Matsushita, "Flux pinning in superconducting 123 materials," *Supercond. Sci. Technol.*, vol. 13, pp. 730–737, 2000.

[4] M. Murakami, D. T. Shaw, and S. Jin, *Processing and Properties of High T_c Superconductors Volume 1, Bulk Materials*, S. Jin, Ed. , New Jersey: World Scientific Publishing Co. Pte. Ltd., 1993.

[5] T. Haugan, P. N. Barnes, I. Maartense, E. J. Lee, M. Sumption, and C. B. Cobb, "Island-growth of $\mathrm{Y_2BaCuO_5}$ nanoparticles in $(211_{\sim 1.5\ \mathrm{nm}}/123_{\sim 10\ \mathrm{nm}}) \times \mathrm{N}$ composite multilayer structures to enhance flux pinning of $\mathrm{YBa_2Cu_3O_{7-\delta}}$ films," *J. Mat. Res.*, vol. 18, pp. 2618–2623, 2003.

[6] T. Haugan, P. N. Barnes, R. Wheeler, F. Meisenkothen, and M. Sumption, "Addition of nanoparticle dispersions to enhance flux pinning of the $\mathrm{YBa_2Cu_3O_{7-x}}$ superconductor," *Nature*, vol. 430, pp. 867–871, 2004.

[7] T. Haugan, P. Barnes, R. Nekkanti, J. M. Evans, L. Brunke, I. Maartense, J. P. Murphy, A. Goyal, A. Gapud, and L. Heatherly, "Deposition of $(211_{\sim 1.0\ \mathrm{nm}}/123_{\sim 10\ \mathrm{nm}}) \times \mathrm{N}$ multilayer coated conductors on Ni-based textured substrates," in *Epitaxial Growth of Functional Oxides, Proceedings of the Electrochemical Society*, A. Goyal, Ed., 2005.

[8] T. J. Haugan, P. N. Barnes, T. A. Campbell, A. Goyal, A. Gapud, L. Heatherly, and S. Kang, "Deposition of $(\mathrm{Y_2BaCuO_5/YBa_2Cu_3O_{7-x}}) \times \mathrm{N}$ multilayer films on Ni-based textured substrates," *Physica C*, vol. 425, pp. 21–26, 2005.

[9] P. N. Barnes, T. J. Haugan, M. D. Sumption, S. Sathiraju, J. M. Evans, and J. C. Tolliver, "$\mathrm{YBa_2Cu_3O_{7-d}}$ films with a nanoparticulate dispersion of $\mathrm{Y_2BaCuO_5}$ for enhanced flux pinning," *Trans. MRS-J*, vol. 29, no. 4, pp. 1385–1388, 2004.

[10] P. N. Barnes, T. J. Haugan, M. D. Sumption, and B. C. Harrison, "Pinning enhancement of $\mathrm{YBa_2Cu_3O_{7-d}}$ thin films with $\mathrm{Y_2BaCuO_5}$ nanoparticulates," *IEEE Trans. Appl. Supercond.*, vol. 15, pp. 3766–3769, 2005.

[11] T. J. Haugan, P. N. Barnes, T. A. Campbell, J. M. Evans, J. W. Kell, L. B. Brunke, J. P. Murphy, C. Varanasi, I. Maartense, W. Wong-Ng, and L. P. Cook, "Addition of alternate phase nanoparticle dispersions to enhance flux pinning of Y-Ba-Cu-O thin films," *IEEE Trans. Appl. Supercond.*, vol. 15, pp. 3770–3773, 2005.

[12] T. J. Haugan, *In-Situ Approach to Introduce Flux pinning in YBCO*, ser. Studies of High Temperatures Superconductors, Book Series, M. Parathaman and V. Selvamanickam, Eds. New York: Nova Sci. Publishers, 2006, submitted for publication.

[13] P. N. Barnes, T. J. Haugan, C. V. Varanasi, and T. A. Campbell, "Flux pinning behavior of incomplete multilayered lattice structures in $\mathrm{YBa_2Cu_3O_{7-d}}$," *Appl. Phys. Lett.*, vol. 18, pp. 4088–4090, 2004.

[14] T. A. Campbell, T. J. Haugan, P. N. Barnes, I. Maartense, J. Murphy, and L. Brunke, "Flux pinning effects of $\mathrm{Y_2O_3}$ nanoparticulate dispersions in multilayered YBCO thin films," *Physica C*, vol. 423, pp. 1–8, 2005.

[15] A. A. Gapud, D. Kumar, S. K. Viswanathan, C. Cantoni, M. Varela, J. Abiade, S. J. Pennycook, and D. K. Christen, "Enhancement of flux pinning in $\mathrm{YBa_2Cu_3O_{7-\delta}}$ thin films embedded with epitaxially grown $\mathrm{Y_2O_3}$ nanostructures using a multi-layering process," *Supercond. Sci. Technol.*, vol. 18, pp. 1502–1505, 2005.

[16] J. Hänisch, C. Cai, R. Hühne, L. Schultz, and B. Holzapfel, "Formation of nanosized $\mathrm{BaIrO_3}$ precipitates and their contribution to flux pinning in Ir-doped $\mathrm{YBa_2Cu_3O_{7-\delta}}$ quasi-multilayers," *Appl. Phys. Lett.*, vol. 86, pp. 122508–122510, 2005.

[17] J. L. MacManus-Driscoll, S. R. Foltyn, Q. X. Jia, H. Wang, A. Serquis, L. Civale, B. Maiorov, M. E. Hawley, M. P. Maley, and D. E. Peterson, "Strongly enhanced current densities in superconducting coated conductors of $\mathrm{YBa_2Cu_3O_{7-x}} + \mathrm{BaZrO_3}$," *Nature Materials*, vol. 3, pp. 439–441, 2004.

[18] A. Goyal, S. Kang, K. J. Leonard, P. M. Martin, A. A. Gapud, M. Varela, M. Paranthaman, A. O. Ijaduola, E. D. Specht, J. R. Thompson, D. K. Christen, S. J. Pennycook, and F. A. List, "Irradiation-free, columnar defects comprised of self-assembled nanodots and nanorods resulting in strongly enhanced flux-pinning in $\mathrm{YBa_2Cu_3O_{7-\delta}}$ films," *Supercond. Sci. Tech.*, vol. 18, pp. 1533–1538, 2005.

[19] S. Kang, A. Goyal, J. Li, A. A. Gapud, P. M. Martin, L. Heatherly, J. R. Thompson, D. K. Christen, F. A. List, M. Paranthaman, and D. F. Lee, "High-performance high- $\mathrm{T_c}$ superconducting wires," *Science*, vol. 311, pp. 1911–1914, 2006.

[20] P. N. Barnes, J. W. Kell, B. C. Harrison, T. J. Haugan, C. V. Varanasi, M. Rane, and F. Ramos, "Minute doping with deleterious rare earths in $\mathrm{YBa_2Cu_3O_{7-\delta}}$ films for flux pinning enhancements," *Appl. Phys. Lett.*, vol. 89, pp. 012503–012505, 2006.

[21] Y. Yoshida, K. Matsumoto, M. Miura, Y. Ichino, Y. Takai, A. Ichinose, M. Mukaida, and S. Horii, "Controlled nanoparticulate flux pinning structures in $\mathrm{RE_{1+x}Ba_{2-x}Cu_3O_y}$ films," *Physica C*, vol. 445–448, pp. 637–642, 2006.

[22] T. Haugan, P. N. Barnes, L. Brunke, I. Maartense, and J. Murphy, "Effect of $\mathrm{O_2}$ partial pressure on $\mathrm{YBa_2Cu_3O_{7-x}}$ thin film growth by pulsed laser deposition," *Physica C*, vol. 297, pp. 47–57, 2003.